Available online at www.sciencedirect.com
SCIENCE DIRECT®
Journal of Magnetic Resonance 181 (2006) 119–125
JMR Journal of Magnetic Resonance
www.elsevier.com/locate/jmr

Fast magnetic resonance imaging and velocimetry for liquids under high flow rates

Petrik Galvosas *, Paul T. Callaghan

MacDiarmid Institute for Advanced Materials and Nanotechnology, School of Chemical and Physical Sciences, Victoria University of Wellington, PO Box 600, Wellington, New Zealand

Received 24 January 2006; revised 18 March 2006
Available online 27 April 2006

Abstract

We here demonstrate the use of NMR velocity imaging techniques to measure flow in a free falling jet of water at speeds up to and on the order of 1 m/s. In particular, we show how to adapt the RARE imaging method, based on a CPMG multiple rf pulse train, so that the real and imaginary parts of the signal may be suitably acquired, enabling pulsed gradient spin echo encoding for flow. We term this method "soft-pulse-quadrature-cycled PGSE-RARE" or SPQC-PGSE-RARE. We further demonstrate the use of a one-dimensional (slice selective) imaging method which takes advantage of the cylindrical symmetry of the flow, and considerably shortens the image acquisition time.

PACS: 47.15.Uv; 47.80.Cb; 76.60.Pc; 82.56.Jn

Keywords: Liquid jet; NMR velocimetry; Fast imaging; Laminar flow

1. Introduction

NMR velocimetry has proven of considerable use as a tool for fluid mechanics investigations. Both the Lagrangian and Eulerian perspectives are available, using pure pulsed gradient spin echo encoding in the former case, and velocity imaging in the second. Ideally, velocity imaging allows one to determine the spatially dependent flow field $\boldsymbol{u}(\boldsymbol{r}, t)$ of the fluid under study where $\boldsymbol{u}(\boldsymbol{r}, t)$ is the velocity at each individual point in space (in the Eulerian picture). This simplifies to $\boldsymbol{u}(\boldsymbol{r})$ in case of a stationary flow where the velocity is time independent. Of course in practice, the resolution of velocity imaging may be limited, either by signal-to-noise or gradient strength availability in the case of spatial coordinates, or by the finite time needed for position encoding in the case of temporal information. It is the latter limitation which concerns us in this paper, where we address the subject of NMR velocimetry in rapidly flowing liquids.

The goal of our investigation is to study a free liquid jet. The knowledge of its flow field and the changes to that flow introduced by added surfactants permits a study of a phenomenon known as the "Marangoni effect" [1]. The technique demonstrated here is aimed at a study of this effect via the changes of the properties of the liquid jet and, in particular, its dependency on the type of surfactant and its concentration. The results of these experiments in regard to the fluid dynamical properties will be published elsewhere. In contrast, the focus of this present article concerns the different NMR pulse sequences that are shown to accomplish the monitoring of liquids in an approximately stationary flow field under flow rates of $\approx$500 mm/s where "flow rate" describes here the spatially dependent time invariant velocity $\boldsymbol{u}(\boldsymbol{r})$ within the flow field. Subsequently, the mean or averaged flow rate describes the averaged velocity $\bar{\boldsymbol{u}} = \int_A \boldsymbol{u}(\boldsymbol{r})\mathrm{d}\boldsymbol{r} / \int_A \mathrm{d}\boldsymbol{r}$ of the liquid flowing through a certain plane A. The challenge for these measurements is twofold. First, the high velocity results in a limited time during which

* Corresponding author. Fax: +49 341 9732549.
E-mail address: galvosas@physik.uni-leipzig.de (P. Galvosas).

1090-7807/$ - see front matter © 2006 Elsevier Inc. All rights reserved.
doi:10.1016/j.jmr.2006.03.020

the spins stay in the rf-coil. Second, we have to deal with fluctuations of the free jet. This means that even in the case where we attempt to establish a stationary flow field (laminar flow), the whole jet jitters slightly thus placing some constraints on the pulse sequences used. Measurements in a rigid geometry such as pipes are therefore much easier to handle even in cases of high velocities.

Velocity profiles have been measured using NMR on various samples and over a wide range in velocity [2–9]. The very first experiment was performed by Hayward and Packer [10] who used pulsed gradient spin echo (PGSE) NMR encoding to deduce the distribution of velocities, without directly obtaining an image. Early NMR microscopy experiments on pipe flow were performed by Callaghan et al. [11]. In this article we shall be concerned with rapid velocimetry, and amongst the fastest known imaging techniques is RARE [12]. Scheenen et al., used the rapid imaging method RARE [12] combined with both pulsed gradient stimulated echo (PGSTE) encoding [13] and a modified PGSE encoding [14] for the investigation of flow processes. However, they studied the water uptake in plant stems e.g., liquids under very small flow rates (on the order of ≈0.5 mm/s). Sederman et al. [15] investigated pipe flow with a SEMI-RARE sequence, without PGSE encoding. In their work the flow profile is directly obtained by acquiring successive NMR images and by employing the image contrast introduced by different fluids having different T_2. These authors measured velocities ≈40 mm/s. Han et al. [16] studied the rheology of blood in pipes of various diameters. They obtained projections of velocities in 1D profiles as well as 1D velocity distributions with maximum velocities of up to 3.5 m/s. Xia and Callaghan [17] used a similar setup and geometry to the setup in this work. They determined the velocity field in a visco-elastic liquid building up a tubeless siphon.

We describe two approaches to imaging rapid flow in this paper. Both are based on a PGSE pulse sequence used to phase encode for the velocity. This phase is introduced into the NMR signal in proportion to the applied magnetic field gradient amplitude g and is given by the expression

$$\exp\{-\mathrm{i}2\pi \boldsymbol{q}\cdot\boldsymbol{u}\Delta\} \quad \text{with} \quad \boldsymbol{q}=\tfrac{1}{2\pi}\gamma\delta\boldsymbol{g}, \tag{1}$$

where δ is the duration of the gradient pulse, Δ is the observation time, γ is the gyromagnetic factor and $\boldsymbol{q}$ is the scattering wave vector (see Fig. 3 for details of the timing). Subsequent Fourier transformation of the acquired NMR signal with respect to $\boldsymbol{q}$ delivers the propagator $\bar{P}(\Delta\boldsymbol{r},\Delta)$, depending on the displacement $\Delta\boldsymbol{r}$. In particular, due to the experimental setup with $\boldsymbol{q}=(0,0,q_z)$, we obtain $\bar{P}(\Delta z,\Delta)$ depending on Δz as the displacement in z-direction and hence, when we combine this encoding with some imaging modality, we are able to obtain u_z at each point of the image (see [18]).

The first pulse sequence to be described employs the RARE sequence in which a prior PGSE segment is used for the velocity encoding. Conventional wisdom has it that such encoding is difficult since the (multi-echo) RARE sequence delivers the real part of the NMR signal unscathed while the imaginary part suffers artifactual attenuation due to rf pulse errors. We shall show later how we address this problem. In the meantime, we note that the RARE approach allows us to measure two-dimensional velocity profiles and was used in experiments with velocities of up to ≈50 mm/s. Although this pulse sequence is very useful for velocities in this range, the velocities occurring in a free liquid jet are much higher. Therefore a second, much simpler, pulse sequence is described here that is used to measure the velocity in only a small strip of the sample, thus providing a one-dimensional velocity profile. Of course, for a liquid jet of circular cross section, this limitation to 1D is not a disadvantage, since the rotational symmetry of the jet should not require a full two-dimensional velocity map. A similar approach was used by Dusschoten et al. [19] for the measurement of displacements in soil model systems.

2. Experimental

All experiments were carried out on a Bruker AMX NMR system at a ^{1}H frequency of 300.14 MHz. The magnet was equipped with a Bruker three axis micro imaging system "Micro 2.5" that provides gradients of up to 1 T/m. The rf resonator used for all experiments has a inner diameter of 15 mm and a height of 20 mm. A glass tube with an outer diameter of 15 mm and an inner diameter of 13.5 mm was fitted right through the resonator providing a "wettable" environment within the magnet.

Two experimental setups were used, one for investigation of the free jet and the other, a less demanding pipe flow for testing of the pulse sequences. For investigation of the free jet, a capillary with inner radius $R=2$ mm was placed in the magnet in such a way that the lower end of the capillary, and hence the upper end of the free liquid jet, is adjusted to the upper end of the rf resonator (see Fig. 7 for a longitudinal section of the jet). A constant laminar flow in the feed pipe was maintained through the use of a gear pump (Cole–Parmer digital dispensing drive with pump head from Micropump, type 184). The jet was captured in a fluid reservoir 50 mm below the end of the capillary i.e., the jet was free for a length of 50 mm without break up. Suppressing the break up by catching the jet in a liquid reservor minimizes spatial fluctuations. A remaining fluctuation, referred to above as "jitter," was observed and just visible with the naked eye. It is a sudden horizontal movement of the jet which occasionally happens on a time scale of several seconds. This setup resulted in an averaged flow rate of $\bar{u} \geqslant 100$ mm/s. Because of

$$u(r)=u_{\max}[1-(r/R)^2] \quad 0\leqslant r\leqslant R \tag{2}$$

for a parabolic laminar flow in a capillary, where $u_{\max}=2\bar{u}$ is the maximum velocity and r the radius, velocities of at least 200 mm/s need to be measured. This consideration

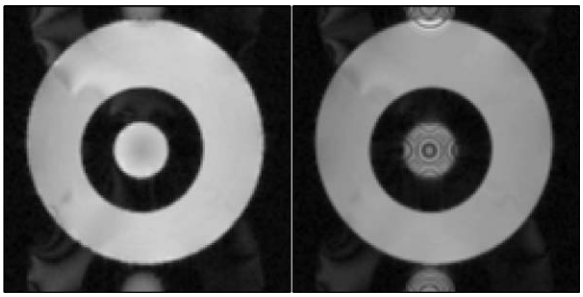

Fig. 1. Image of the test setup (capillary with $R = 1.45$ mm) at $q = 0$ (left) and $q = 11.7\ \mathrm{mm}^{-1}$ (right) using the RARE pulse sequence with hard pulses at $\bar{u} = 10.6$ mm/s.

of course neglects the increasing velocity in the free jet due to gravitation. Thus, we have to expect even higher velocities downstream.

The second test setup was less demanding in respect of the flow field to be maintained, and was used for testing the pulse sequences. For this purpose a capillary with inner radius $R = 1.45$ mm or $R = 2$ mm was fitted vertically right through the rf resonator allowing the measurements of pipe flow without restrictions. In the same setup, the water level in the reservoir was moved up filling up the resonator and surrounding the capillary, thus providing a bulk fluid under rest as a reference (see Fig. 1 for a cross section with the stationary liquid surrounding the moving one in the middle).

The first attempt to obtain velocity maps utilised the combination of a PGSE pulse sequence with a traditional spin warp imaging pulse sequence (see [18]). Hence, the acquisition of one image is carried out over several excitations while stepping the phase gradient. Because of the aforementioned spatial fluctuations of the free liquid jet the coherence of the signal in the phase direction is severely disturbed, leading to distorted images after the Fourier transformation. It became apparent that only fast imaging techniques could overcome this problem, i.e., where the image is acquired in a time short compared to the time of the spatial fluctuations of the jet. We therefore set out to use a pulse sequence where a PGSE and RARE sequence is combined.

2.1. Two-dimensional velocity mapping with RARE

We developed a pulse sequence for a two-dimensional velocity mapping which is based on that published by Scheenen et al. [14] (although in our case, the sampling of k-space in the phase direction was changed to a progressive scheme from $k_p^{\min}$ to $k_p^{\max}$). We have found that the use of hard π-pulses in the RARE part of the pulse sequence led to significant artifacts in which a part of the intensity in the central part of the image, where flow occurs, is transferred to the image border, a classic phase encoding "ghosting" associated with $\pm$ signal modulation with respect to the successive phase steps. The intensity of this artifact depends on the velocity encoding gradient strength applied as well as on the velocity of the fluid itself. In other words it depends on the phase shift given by Eq. (1). These artifacts are a consequence of the imaging process, adding flow and q gradients merely enhances them. In Fig. 1 the left image is acquired with a velocity of $\bar{u} = 10.6$ mm/s and $q = 0$. A slight ghosting for both the moving and stationary parts of the image is observed. However, when the image is acquired at the same flow rate but at $q = 11.7\ \mathrm{mm}^{-1}$ ($\delta = 1$ ms, $g = 0.274$ T/m) (right hand image) a more severe ghosting occurs for the part of the image associated with moving fluid. The explanation for these effects is obvious and as old as the original paper by Carr and Purcell [20] who noted that odd and even echoes alternate in amplitude due to rf pulse imperfections, while flow induces even more severe odd-even alternation. It is exactly this modulation which leads to the ghosts (see e.g., [21], the explanation given there applies also for RARE), and more severely so for the flowing liquid. These "ghosting" artifacts, including the PGSE-induced intensity modulation visible for the liquid under flow in the right image in Fig. 1, can thus be largely reduced by the use of only the even echos within the RARE part of the pulse sequence. The price one needs to pay is a double duration pulse sequence. Considering the limited time the spins stay in the resonator this is a severe limitation. Furthermore, the acquired NMR signal reduces due to T_2 relaxation.

In addition to the ghosting, the imaginary part of the NMR signal tends to be lost during the execution of the RARE part of the pulse sequence, a general feature of pulse sequences based on the Carr–Purcell–Meiboom–Gill (CPMG) sequence [22]. This problem is not necessarily fatal, but is certainly inconvenient. The loss of the imaginary signal leads to a symmetrical positive and negative flow mirroring of the propagator in the subsequent Fourier transformation of the acquired data with respect to the q-direction, as the input data are no longer modulated by an exponential function with a complex argument but instead experience a cosine modulation. While such mirroring may be acceptable at large propagator displacements, at low velocities it leads to overlap distortions.

We tried several strategies in an attempt to overcome this loss of the imaginary signal as well as the suppression of the ghost artifacts. Neither the applying of longer phase cycles as described in [23] nor the usage of crusher gradients as it is described in [14] led to a satisfactory result. Two changes enabled the RARE imaging sequence with PGSE velocity encoding to work well in acquiring velocity maps. First, we replaced the hard pulses in the RARE part by soft pulses (see Fig. 3). The corresponding slice gradient was reduced to such a degree that the whole resonator length is included in the slice selected i.e., the molecules do not move out of the slice while acquiring the image. Moreover, this way any successive narrowing of the slice is circumvented. Remarkably, this approach caused a significant reduction in ghosting artifacts by comparison with that found when using hard pulses as shown in Fig. 2. No ghosting and no modulation of the signal is apparent

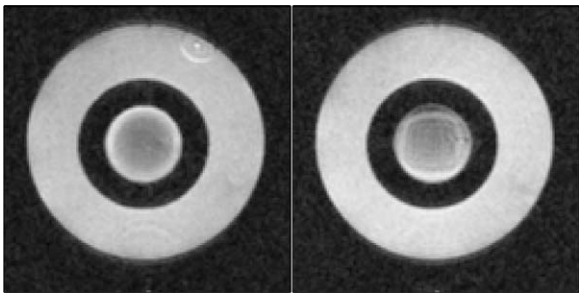

Fig. 2. Image of the test setup (capillary with $R = 2$ mm) at $q = 0$ (left) and $q = 8.75\ \mathrm{mm}^{-1}$ (right) using the RARE pulse sequence with soft pulses at $\bar{u} = 33.4$ mm/s.

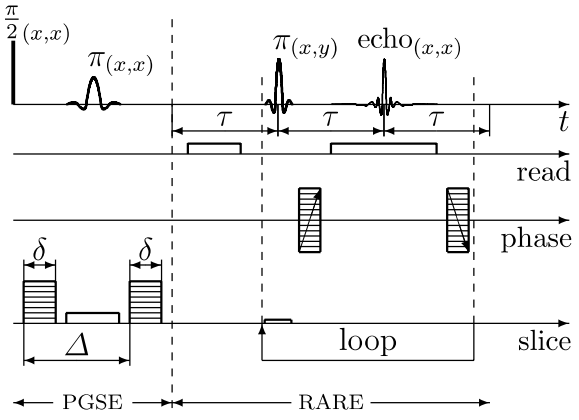

Fig. 3. Pulse program for the velocimetry experiment with RARE using soft pulses within the RARE part. Note the shorter, more intense soft pulses in conjunction with a smaller slice gradient as well as the phase scheme in the RARE part.

although the flow rate is about three times higher than the setup used for Fig. 1, which in turn also means no odd/even echo modulation is introduced by the weak slice gradients in the echo train. As before it is $q = 0$ at the left hand side image, while it is $q = 8.75\ \mathrm{mm}^{-1}$ ($\delta = 1$ ms, $g = 0.206$ T/m) at the right hand side image.

This presumed reduction in odd/even echo amplitude modulation necessarily arises because the restriction of the excitation to the region inside the rf coil results in a more uniform rf excitation across the sample. Note that the power of the soft pulses in the RARE part was chosen to be the maximum available to keep the rf pulse duration and hence the whole pulse sequence as short as possible.

To avoid the cosine modulation effect and restore the full complex signal, we used the phase cycle indicated in Fig. 3. It is similar to the one used by Perlo et al. [24] to increase the signal-to-noise ratio by acquiring a CPMG echo train and subsequent adding of the echos. The full phase cycle is extended by a compensation (add/subtract) cycle and given in Table 1.

While the phase of the preparation as well as the detection of the spin system is the same for each phase step (the phase of the first π pulse is always x) the phase of the π pulse train switches between x and y. It is known that the magnetization in a CPMG train is preserved in the

Table 1
Phase cycle for the pulse sequence with RARE

π/2	π (1st slice)	π (train)	Acquisition
x	x	x	x
x	x	y	x
$-x$	x	x	$-x$
$-x$	x	y	$-x$

direction of the rf pulse applied. Therefore with the phase of the π pulse in the first phase step set to x it is the signal along x which is preserved and acquired within the echo train. The signal along y decays rapidly and does not contribute at the center of the k space (in the middle of the echo train). During the second phase step the phase of the π pulses in the echo train is set to y which means the signal along y is acquired while the signal along x decays rapidly. This way with every even number of phase steps the whole complex NMR signal is accumulated in the acquisition memory. Phase step three and four repeat the same scheme while compensating baseline errors.

The application of the above phase cycle, in conjunction with the use of soft pulses within the RARE echo train provides the key to the acquisition of an undistorted two-dimensional image containing the correct phase information arising from the successively increased PGSE gradient pair. It is suitable for a subsequent Fourier transformation with respect to q in each voxel and hence the accurate determination of the propagator in each voxel. The RARE pulse sequence with preceding PGSE gradients described above proved to be highly successful in the spatial mapping of the velocities derived from the individual propagators for the laminar flow in a pipe as we will show in the results section. This sequence is fast enough to suppress the influence of the spatial fluctuation with respect to the imaging phase gradient. We term this method "soft-pulse-quadrature-cycled PGSE-RARE" or SPQC-PGSE-RARE.

However, considering the fact that we have to apply soft pulses within the RARE part instead of hard pulses, a single scan runs for 100 ms or longer if one wishes to achieve a reasonable resolution. Given the rf coil geometry with a length of 20 mm this limits the peak velocity to $u = 200$ mm/s or even less. This corresponds to the required minimal peak velocity of the water at the nozzle as discussed earlier. Of course there is a strong influence of gravity on the jet accelerating the center of the jet towards much higher velocities. For this particular experimental setup the pulse sequence employing RARE is less attractive. Therefore, we had to find a different solution for the free liquid jet, even though the pulse sequence using RARE works very well for velocities of the order of 100 mm/s.

2.2. One-dimensional velocity mapping

A simple "speed-up" solution is to remove the loop of the RARE sequence and insert a second slice gradient instead of the phase gradient as shown in Fig. 4. This

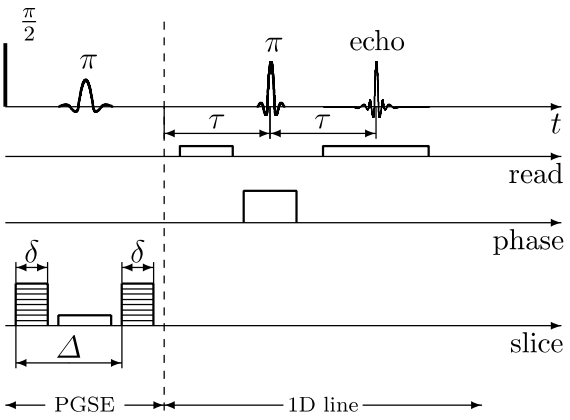

Fig. 4. Pulse program for the velocimetry experiment with 1D imaging using two slice gradients. Note the intensity ratio of the first and second slice gradient.

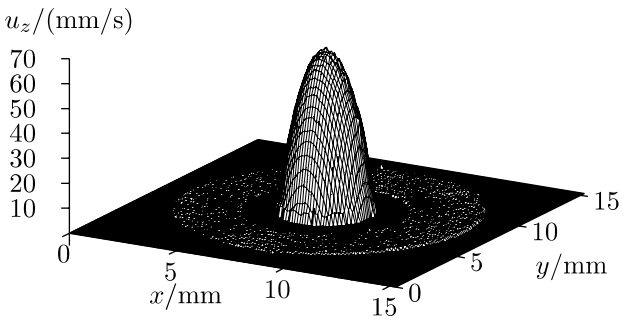

Fig. 5. Two-dimensional velocity profile of pipe flow acquired with the pulse sequence using "soft-pulse-quadrature-cycled" PGSE-RARE (SPQC-PGSE-RARE) (see Fig. 3). Note the stationary fluid surrounding the capillary. See text for experimental details.

reduces the dimension of the measurement by one, i.e., from two-dimensional to one-dimensional. The advantage of this change is the gain in speed, the disadvantage the loss of information. In this particular case this is not a severe drawback provided that the velocity profile is acquired across the center line of the jet in accordance with the rotational symmetry of the object under study. It is therefore apparent that the second slice needs to be thin compared to the diameter of the jet keeping the velocity distribution small within one voxel.

To find the three-dimensional flow field one needs to carry out several measurements at different distances from the end of the nozzle (different offset frequencies with respect to the first slice gradient).

The pulse sequence modified this way is able to run below 10 ms. Therefore, it seems to be possible to measure velocities well above 0.5 m/s considering the length of the rf resonator. In contrast to [16] we observe discrete velocities for each individual voxel leading to an unambiguous velocity profile independent from the shape of the sample cross section. While this makes the pulse sequence more robust the penalty to be paid is a slightly longer pulse sequence due to the second slice gradient introduced. The spatial fluctuations of the jet, breaking the rotational symmetry in general, do not exceed one voxel size. A distortion of the velocity phase encoding is therefore not considered to be severe and is further reduced by signal accumulation within one q gradient step.

3. Results

3.1. Pipe flow velocity profiles

Fig. 5 shows the two-dimensional laminar flow field of a pipe flow with a capillary of $R = 2$ mm and $\bar{u} = 33.4$ mm/s adjusted at the gear pump. The peak velocity measured in the middle of the pipe with $u_{\max} = 65$ mm/s is in a good agreement to the mean flow rate. For this measurement the simple pipe flow test setup was used as described earlier with the slice selected at the upper end of the resonator. One can clearly see the fluid under rest surrounding the capillary at velocities of ≈ 0 mm/s (compare Fig. 1). The field of view acquired is (15.36×15.36) mm^2 with a spatial resolution of (120×120) μm^2 which corresponds to 128×128 pixels. The chosen slice thickness is 1 mm. The observation time in the PGSE part is $\Delta = 5$ ms with a gradient width of $\delta = 1$ ms. Eight q gradient steps were used up to a maximum gradient intensity of $g_{\max} = 0.206$ T/m allowing a maximum velocity of 80 mm/s to be measured.

Using the highest available spectral width of 125 kHz (under a read gradient of 0.19 T/m) as well as a high maximum phase gradient of 0.76 T/m (81% of the maximal gradient provided by the instrument) the echo distance in the RARE part is $2\tau = 2.4$ ms. Including the time of the PGSE part and considering the fact that the loop in the RARE part is 128 times executed the length of the pulse sequence is 323 ms (this is still short compared to the T_2 of free water, hence we do not expect image artifacts due to convolution of the signal intensity in the phase direction with T_2). This leads to a displacement of the water molecules in the center of the pipe of $\Delta z = 21$ mm which is the length of the rf resonator. Therefore, for the given experimental setup (velocity, field of view, position of the slice and resolution), this measurement is at the upper limit of the method. In fact, as one can see from Fig. 2, there is a loss of intensity which depends on the velocity of the spins. As expected, the fastest spins are affected the most. However, the pulse sequence proves to be robust and reliable within the limits as the drop in intensity is not severe and does not affect the acquired velocity map.

A single velocity profile acquired with the 1D imaging pulse sequence across the center line of the capillary ($R = 2$ mm) is shown in Fig. 6. The field of view is chosen to be 12.8 mm with a resolution of 100 μm (128 pixel). The first slice (perpendicular to the direction of the flow) is 1 mm thick while the second slice selects only 200 μm. The observation time used in this experiment is $\Delta = 2$ ms with $\delta = 190$ μs. Eight q gradient steps were used up to a maximum gradient intensity of $g_{\max} = 0.361$ T/m allowing

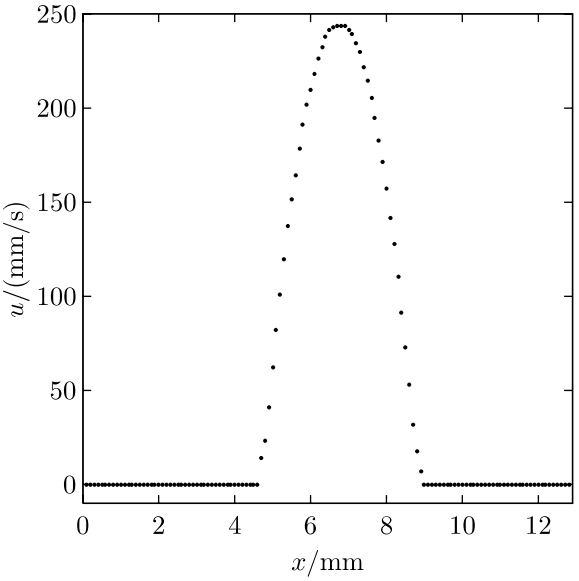

Fig. 6. 1D velocity profile of pipe flow acquired across the center line of the flow. See text for experimental details.

a maximum velocity of 600 mm/s to be measured. The obtained peak velocity of 244 mm/s is in agreement to the mean flow rate of $\bar{u} = 128$ mm/s chosen on the gear pump.

The length of the pulse sequence is 7 ms ($2\tau = 4$ ms). Considering the peak velocity, the displacement during the experiment is only $\Delta z = 1.7$ mm indicating that even 10 times higher velocities might be measurable.

3.2. Liquid jet velocity profile

For the measurement of velocity profiles of the jet we used the pulse sequence shown in Fig. 4 and tested for velocities in a pipe of up to 250 mm/s with similar experimental parameters as reported above. The mean flow rate on the pump was chosen to be $\bar{u} = 192$ mm/s which is well above the required flow rate for a jet without break up. Since the flow field is not invariant in respect to z, the slice thickness in flow direction was reduced to 500 μm leading to a voxel size of $(100 \times 200 \times 500)$ μm^3. To keep the influence of the motion small during acquisition we used the maximal available spectral width of 125 kHz leading to an acquisition period of 1.024 ms for a resolution of 128 pixels. At the nozzle, the maximum displacement during acquisition is about 0.4 mm which is less than the slice thickness. Further down the jet, where the diameter change is less severe, the displacement is still in the range of the slice thickness (0.6 mm). In fact we did not observe any distortion due to the motion during acquisition. Fig. 7 shows a corresponding NMR intensity map of in total 21 measurements carried out at different distances from the end of the nozzle, e.g., at $\Delta z = (0, 1, 2, \ldots, 20)$ mm. The position of the second slice (across the jet) was determined by the acquisition of a 2D image with the RARE part of the SPQC-PGSE-RARE sequence with a slice taken at

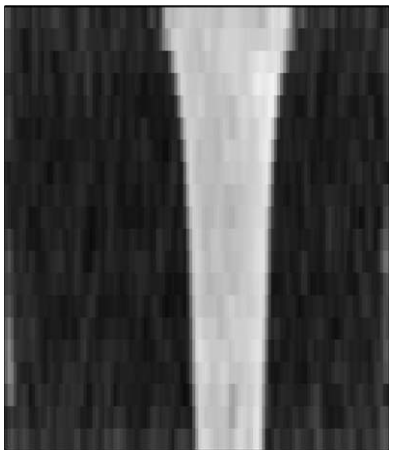

Fig. 7. NMR image of the water jet. Each row represents an individual measurement carried out with the pulse sequence shown in Fig. 4. The voxel size is $(100 \times 200 \times 500)$ μm^3 and the width and hight of the image (12.8×20) mm^2 respectively.

the end of the nozzle. The slower spins are visible in the image as a ring from which the optimal position of the second slice in the 1D sequence can be conveniently derived.

Due to the higher initial velocity and the acceleration due to gravity the maximum q gradient was reduced to 0.24 T/m. This allowed us to measure a maximum velocity of 900 mm/s. The velocity map obtained is shown in Fig. 8.

As before, the peak velocity at the center line at $\Delta z = 0$ is in good agreement with the mean flow rate chosen at the pump. Moreover, for each individual slice the mean flow rate can be calculated in cylindrical coordinates with

$$\bar{u} = \frac{\int_{x_0-R}^{x_0+R} u(x - x_0)(x - x_0)\mathrm{d}x}{R^2}, \tag{3}$$

where x_0 is the center and R the radius of the jet at the corresponding distance from the nozzle respectively (see scatter graph in Fig. 9). The result returns $\langle \bar{u} \rangle = (192 \pm 19)$ mm/s where $\langle \bar{u} \rangle$ is the averaged value out of the 21 calculated mean flow rates (see solid line in Fig. 9) and the error given the largest absolute deviation from the mean value. As one can see clearly from Fig. 9 the calculated mean flow rate is constant as required to satisfy

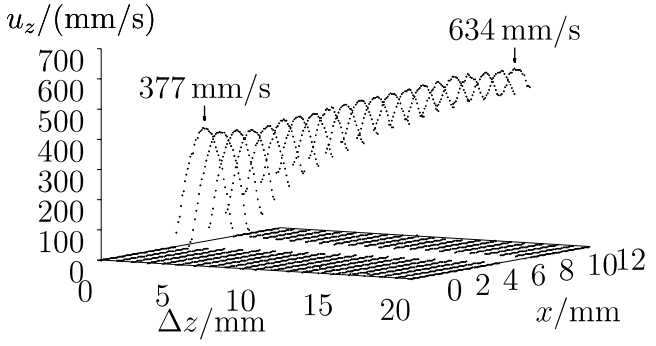

Fig. 8. Velocity map of the water jet at an averaged flow rate of $\bar{u} = 192$ mm/s.

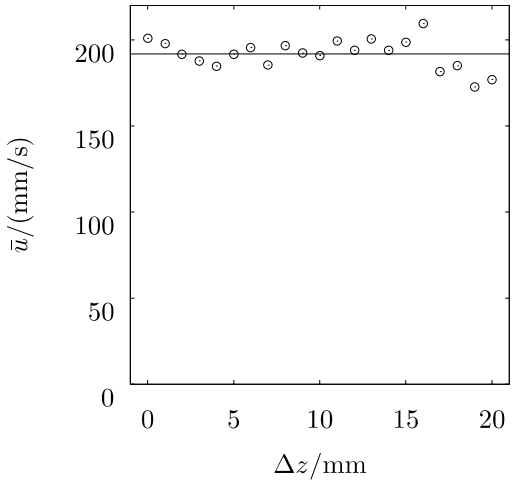

Fig. 9. Mean flow rate for each individual velocity profile taken as shown in Fig. 8. The solid line is the average of the 21 mean flow rates.

conservation of the volume flow rate. Compared to the nominal averaged flow rate chosen at the pump the averaged value $\langle\bar{u}\rangle$ is in excellent agreement and the error moderate considering the spatial resolution compared to the size of the jet especially for large distances from the nozzle.

4. Conclusions

We have demonstrated two NMR imaging pulse sequences suitable for the measurement of flow fields at relatively high flow rates, and under conditions where the flow field may fluctuate. The first pulse sequence (SPQC-PGSE-RARE) is based on the combination of a PGSE encoding and suitably modified RARE imaging, and allows the measurement of two-dimensional velocity profiles. Given an rf resonator length of 20 mm we acquired velocities of up to 65 mm/s at a spatial resolution of (120×120) μm (128×128 pixels). By reducing the field of view and/or the resolution, higher velocities might easily be measured.

The second pulse sequence uses a one-dimensional imaging sequence. Reducing the dimension by one shortens the length of the pulse sequence tremendously. Hence, the velocity able to be observed is increased significantly (as is any fluctuation time). The reduction of the dimension and subsequent loss of information is not necessarily a concern for systems with a corresponding symmetry. For the sample under study, the free liquid jet, cylindrical symmetry is available and a flow field with discrete velocities per voxel of up to 634 mm/s was acquired.

Both pulse sequences turn out to be robust and reliable and proved to be useful for the investigation of pipe flow as well as free liquid jets.

Acknowledgments

We gratefully acknowledge financial support by the New Zealand Centres of Research Excellence Fund, the New Zealand Foundation for Research, Science and Technology, and the Royal Society of New Zealand Marsden Fund. We thank Alexandre Khrapitchev for the helpful discussions regarding the two-dimensional RARE pulse sequence.

References

[1] C. Marangoni, über die ausbreitung der tropfen einer flüssigkeit auf der oberfläche einer anderen, Ann. Phys. Chem. 143 (7) (1871) 337.
[2] A. Amar, S. Stapf, B. Blümich, Internal fluid dynamics in levitated drops by fast magnetic resonance velocimetry, Phys. Rev. E. 72 (3) (2005) 030201.
[3] P.T. Callaghan, Rheo-nmr: nuclear magnetic resonance and the rheology of complex fluids, Rep. Prog. Phys. 62 (4) (1999) 599–670.
[4] A.D. Hanlon, S.J. Gibbs, L.D. Hall, D.E. Haycock, W.J. Frith, S. Ablett, Rapid mri and velocimetry of cylindrical couette flow, Magn. Reson. Imaging 16 (8) (1998) 953–961.
[5] C. Heine, K. Kupferschläger, S. Stapf, B. Blümich, Nmr velocimetry of falling liquid films, J. Magn. Reson. 154 (2) (2002) 311–316.
[6] M.R. Lopez-Gonzalez, W.M. Holmes, P.T. Callaghan, P.J. Photinos, Shear banding fluctuations and nematic order in wormlike micelles, Phys. Rev. Lett. 93 (26) (2004) 268302.
[7] X.H. Ren, S. Stapf, B. Blümich, Nmr velocimetry of flow in model fixed-bed reactors of low aspect ratio, AIChE J. 51 (2) (2005) 392–405.
[8] M.D. Mantle, A.J. Sederman, Dynamic mri in chemical process and reaction engineering, Prog. NMR Spectrosc. 43 (2003) 3–60.
[9] E. Fukushima, Nuclear magnetic resonance as a tool to study flow, Annu. Rev. Fluid Mech. 31 (1999) 95–123.
[10] R.J. Hayward, K.J. Packer, D.J. Tomlinson, Pulsed-field-gradient spin echo nmr studies of flow in fluids, Mol. Phys. 22 (1972) 1083–1102.
[11] P.T. Callaghan, C.D. Eccles, Y. Xia, Nmr microscopy of dynamic displacements: *k*-space and *q*-space imaging, J. Phys. E. 21 (1988) 820–822.
[12] J. Hennig, A. Nauerth, H. Friedburg, Rare imaging: a fast imaging method for clinical mr, Magn. Reson. Med. 3 (6) (1986) 823–833.
[13] T.W.J. Scheenen, F.J. Vergeldt, C.W. Windt, P.A. de Jager, H. van As, Microscopic imaging of slow flow and diffusion: a pulsed field gradient stimulated echo sequence combined with turbo spin echo imaging, J. Magn. Reson. 151 (2001) 94–100.
[14] T.W.J. Scheenen, D. van Dusschoten, P.A. de Jager, H. van As, Microscopic displacement imaging with pulsed field gradient turbo spin–echo nmr, J. Magn. Reson. 142 (2000) 207–215.
[15] A.J. Sederman, M.D. Mantle, L.F. Gladden, Single excitation multiple image RARE (SEMI-RARE): ultra-fast imaging of static and flowing systems, J. Magn. Reson. 161 (2003) 15–24.
[16] S.-I. Han, O. Marseille, C. Gehlen, B. Blümich, Rheology of blood by NMR, J. Magn. Reson. 152 (2001) 87–94.
[17] Y. Xia, P.T. Callaghan, Imaging the velocity profiles in tubeless siphon flow by nmr microscopy, J. Magn. Reson. 164 (2003) 365–368.
[18] P.T. Callaghan, Principles of Nuclear Magnetic Resonance Microscopy, Clarendon Press, Oxford, 1991.
[19] D. van Dusschoten, J. van Noort, H. van As, Displacement imaging in porous media using the line scan nmr technique, Geoderma 80 (1997) 405–416.
[20] H.Y. Carr, E.M. Purcell, Effects of diffusion on free precession in nuclear magnetic resonance experiments, Phys. Rev. 94 (1954) 630.
[21] S.M. Grieve, A.M. Blamire, P. Styles, Elimination of nyquist ghosting caused by read-out to phase-encode gradient cross-terms in epi, Magn. Reson. Med. 47 (2002) 337–343.
[22] S. Meiboom, D. Gill, Modified spin–echo method for measurement of relaxation times, Rev. Sci. Instrum. 29 (1958) 688–691.
[23] T. Gullion, D.B. Baker, M.S. Conradi, New, compansated Carr–Purcell sequences, J. Magn. Reson. 89 (1990) 479–484.
[24] J. Perlo, F. Casanova, B. Blümich, 3D imaging with a single-sided sensor: an open tomograph, J. Magn. Reson. 166 (2004) 228–235.